HHS Public Access

Author manuscript

Clin Chim Acta. Author manuscript; available in PMC 2017 July 21.

Published in final edited form as:

Clin Chim Acta. 2016 November 01; 462: 210–214. doi:10.1016/j.cca.2016.09.022.

SLC52A2 [p.P141T] and *SLC52A3* [p.N21S] causing Brown-Vialetto-Van Laere Syndrome in an Indian patient: First genetically proven case with mutations in two riboflavin transporters

Tamilarasan Udhayabanu[a], **Veedamali S Subramanian**[b,c], **Trevor Teafatiller**[c], **Vykuntaraju K Gowda**[d], **Varun S Raghavan**[d], **Perumal Varalakshmi**[a], **Hamid M Said**[b,c], and **Balasubramaniem Ashokkumar**[a,*]

[a]School of Biotechnology, Madurai Kamaraj University, Madurai 625021, India

[b]Departments of Medicine, Physiology/Biophysics, University of California, Irvine, CA 92697, USA

[c]Department of Veterans Affairs Medical Center, Long Beach, CA 90822, USA

[d]Department of Pediatric Neurology, Indira Gandhi Institute of Child Health, Bangalore, India

Abstract

Background—Brown-Vialetto-Van Laere Syndrome (BVVLS), a rare neurological disorder characterized by bulbar palsies and sensorineural deafness, is mainly associated with defective riboflavin transporters encoded by the *SLC52A2* and *SLC52A3* genes.

Methods—Here we present a 16-year-old BVVLS patient belonging to a five generation consanguineous family from Indian ethnicity with two homozygous missense mutations viz., c. 421C>A [p.P141T] in *SLC52A2* and c.62A>G [p.N21S] in *SLC52A3*.

Results—Functional characterization based on ^{3}H-riboflavin uptake assay and live-cell confocal imaging revealed that the effect of mutation c.421C>A [p.P141T] identified in *SLC52A2* had a slight reduction in riboflavin uptake; on the other hand, the c.62A>G [p.N21S] identified in *SLC52A3* showed a drastic reduction in riboflavin uptake, which appeared to be due to impaired trafficking and membrane targeting of the hRFVT-3 protein.

Conclusions—This is the first report presenting mutations in both riboflavin transporters hRFVT-2 and hRFVT-3 in the same BVVLS patient. Also, c.62A>G [p.N21S] in *SLC52A3* appears to contribute more to the disease phenotype in this patient than c.421C>A [p.P141T] in *SLC52A2.*

Keywords

hRFVT-2; hRFVT-3; BVVLS; Motor neuronopathy

*Corresponding author at: Department of Genetic Engineering, School of Biotechnology, Madurai Kamaraj University, Madurai 625 021, India.

Supplementary data to this article can be found online at http://dx.doi.org/10.1016/j.cca.2016.09.022.

Conflict of interest

Authors confirm that this article content has no conflict of interest.

1. Introduction

Brown-Vialetto-Van Laere Syndrome is a neurodegenerative disorder characterized by sensorineural deafness, respiratory difficulty, ponto bulbar palsy and muscle weakness due to the involvement of cranial nerves VII, IX and XII [1]. This rare neurological disorder is mostly regarded as autosomal recessive and rarely as autosomal dominant and X-linked inheritance [2]. Recent findings suggest that the severity of this disease is related to riboflavin (RF) deficiency, caused by a defect(s) in either the *SLC52A2* (OMIM: 607882) or the *SLC52A3* (OMIM: 613350) genes that encode RF transporters 2 & 3 (RFVT-2 and RFVT-3), respectively [1,3]. Three RF transporters namely *SLC52A1*/*hRFVT-1* (NM_017986), *SLC52A2/hRFVT-2* (NM_033409) and *SLC52A3/hRFVT-3* (NM_024531) have been identified in humans and are distributed in a tissue-specific manner [4,5]. The protein sequence of *SLC52A1* is 86.7% identical with that of *SLC52A2* and 44.1% with that of *SLC52A3* [4].

Riboflavin (vitamin B2), a water soluble vitamin is essential for normal cellular functions in its biologically active forms (FMN and FAD), which act as intermediaries in the transfer of electrons in biological oxidation-reduction reactions. Riboflavin transporters (RFVT) play an essential role in the maintenance of RF homeostasis through its absorption in the intestine and reabsorption in the kidney. Several loss-of-function mutations have been identified in *SLC52A2* or *SLC52A3* genes from patients with motor neuron diseases or neuranopathies [1,3,6,7], while mutations in *SLC52A1* have been correlated with glutaric aciduria [8]. The identification of such clinical mutations in *RFVT* genes has led to a better understanding of the pathophysiology of associated neurological disorders and further guided disease management in the affected patients by RF supplementation [9]. In this study, our mutational analysis in a BVVLS patient from Indian ethnicity had identified two homozygous mutations from two different riboflavin transporter encoding genes *SLC52A2* (c.C421A; p.P141T) and *SLC52A3* (c.A62G; p.N21S), which were functionally defective in riboflavin transport activity. Such an identification of clinical mutations in both RF transporters *SLC52A2* and *SLC52A3* in a BVVLS patient has been reported for the first time and not been previously reported elsewhere in any ethnicity.

2. Materials and methods

2.1. Clinical testing

All the genetic investigations were performed after getting informed consent as approved by Institutional Ethical Committee of Madurai Kamaraj University, Madurai, India. Blood samples were collected from a 16-year-old BVVLS patient who belongs to a five-generation consanguineous Indian family at Indira Gandhi Institute of Child Health, Bangalore. Detailed clinical records of medical history and scientific examinations were made.

2.2. Genetic testing/mutation screening

DNA was isolated from whole blood using HiPurA blood genomic DNA isolation kit. Polymerase chain reaction was performed to scan for mutations in *SLC52A2* and *SLC52A3* using specific primers designed in intron-exon boundaries (Supplementary Table 1). All 8

exons were sequenced bidirectionally and compared with wild-type *SLC52A2* and *SLC52A3* genes respectively.

To determine the co-segregation of the identified missense mutations that produced either a loss or gain of a restriction site, RFLP analysis was performed with a 219 bp region spanning exon-3 of *SLC52A2* and a 716 bp region spanning exon-2 of *SLC52A3* using specific enzymes *TspRI* and *MnlI*, respectively. The fragments were separated in 12% poly-acrylamide gel to differentiate wild-type and mutant alleles. A healthy volunteer donor without a history of BVVLS served as a control.

2.3. In silico analysis

To determine the location of the identified clinical mutations, transmembrane topology of hRFVT-2 and hRFVT-3 was predicted using TMHMM (http://www.cbs.dtu.dk/services/TMHMM/). Pathogenicity of the missense mutations was analyzed using the *in silico* tools Polyphen and Mutation taster. To analyze the conserved nature of the identified clinical mutation, protein sequences of hRFVT-2 and hRFVT-3 from human, cat, dog, and monkey were retrieved from NCBI and multiple sequence alignment was performed.

2.4. Site directed mutagenesis

Site-directed mutagenesis was performed based on *Dpn*I method [10], to generate the mutant constructs using pEGFP-C3-hRFVT-2 and pEGFP-C3-hRFVT-3 as templates with specific mutant primers (Supplementary Table 1).

2.5. Cell culture and transient transfection

Human duodenum adenocarcinoma cells (HuTu-80) and human brain cells (U87) were maintained in DMEM supplemented with 10% FBS, glutamine (0.29 g/L), sodium bicarbonate (2.2 g/L), penicillin (100,000 U/L), and streptomycin (10 mg/L). For RF transport assay, cells were grown in 12-well tissue culture plates and for localization studies, cells were grown in sterile glass-bottomed petri dishes. Cells at 80–90% confluency were transfected with 3 μg of the wild-type and mutant constructs with 3 μL Lipofectamine 2000.

2.6. Riboflavin uptake assay

HuTu-80 cells transfected with wild-type (GFP-hRFVT-2 and GFP-hRFVT-3) and mutant (GFP-hRFVT-2[P141T] and GFP-hRFVT-3[N21S]) constructs of *SLC52A2* and *SLC52A3* were tested for ^{3}H-RF uptake activity by incubating the cells in Krebs-Ringer (KR) buffer containing ^{3}H-RF (14 nM) at 37 °C for 3 min as described previously [11]. Radioactivity was measured using a liquid scintillation counter and normalized with total protein content.

2.7. Live-cell confocal imaging studies

HuTu-80 and U87 cells transfected with wild-type and mutant constructs of hRFVT-2 and hRFVT-3 were imaged using an inverted Nikon C-1 confocal microscopy 24–48 h post transfection as described earlier [11]. Fluorophores were excited using a 488 nm line from an argon ion laser, and emitted fluorescence was monitored with a 530 ± 20 nm band pass (GFP) and the red fluorescent protein (DsRed) was excited with HeNe ion laser at 543 nm.

2.8. Statistical analysis

Data are means ± SE of 3–5 independent experiments. Data were analyzed by one-way ANOVA followed by Tukey's honest significant difference (HSD) test, with statistical significance being set at 0.01 (*$P < 0.01$; **$P < 0.001$).

3. Results

3.1. Clinical observations

The 16-year-old proband of Indian origin was presented with bulbar palsy illness like dysphagia, nasal regurgitation and recurrent aspiration. Respiratory compromise was observed at the age of 9 and deafness was perceived at the age of 11. The patient exhibited typical facial weakness like incomplete closure of eyelids and lower motor neuron limb signs with progressive thinning of muscles. A biochemical profile of the proband showed decreased plasma RF (1.89 μg/L; normal range is 3–15 μg/L) and creatinine levels (0.4 mg/dL; normal range is 0.5–1.5 mg/dL), whereas brain MRI displayed no abnormalities (Fig. 1A). The patient responded well to oral RF supplementation and started to show an improvement in diaphragmatic function by gaining motor function and muscle strength.

3.2. Genetic testing/mutation screening

As a result of mutational screening, two homozygous missense mutations in two different RF transporters were identified in the BVVLS proband. A homozygous novel missense mutation c.C421A; p.P141T was identified in exon-3 of *SLC52A2* and another mutation c.A62G; p.N21S was detected in exon-2 of *SLC52A3*. It is evidenced from the chromatograms that both the mutations were segregated from the parents, as they were heterozygous (Fig. 1B & 1C). The family pedigree illustrates the allelic defect of both the mutations in the affected individuals (Fig. 1D).

RFLP analysis with *Mnl*I and *Tsp*RI for the confirmation of the missense mutation c.C421A in *SLC52A2* and c.A62G in *SLC52A3*, respectively, showed that the proband was homozygous with the elimination of these restriction sites, whereas both the parents were heterozygous due to the presence of both the normal and mutant allele (Fig. 2A & 2B). In addition, the sibling was heterozygous for c.C421A in *SLC52A2*, while there was no variation in *SLC52A3*. The parents and an unaffected sibling of the proband were heterozygous for one or the other mutation, suggesting segregation with disease status within this family and autosomal recessive inheritance.

3.3. In silico analysis

Transmembrane topology predictions using TMHMM for both the hRFVT-2 and hRFVT-3 suggested 11 transmembrane domains (TMD) with the amino terminal facing the cytoplasm while the carboxy terminal pointing towards the cell exterior. According to these predictions, proline at 141th position appears to be located in the 2nd intracellular loop of hRFVT-2 between TMDs 4 and 5 while asparagine at 21st position is located in the 1st TMD of hRFVT-3.

Functional consequences of the identified clinical mutations were predicted using Polyphen and Mutation taster. As a result, Polyphen analysis showed that p.P141T is possibly damaging to the structure with a score of 0.954, and p.N21S is probably damaging with a score of 1.0 (Fig. 2C). Mutation taster analysis revealed that both the wild-type amino acid residues in hRFVT-2 and hRFVT-3 mutated in the pro-band were highly conserved and these mutations were predicted to be disease causing with splice site changes (Fig. 2D).

3.4. Riboflavin uptake assay

^{3}H-RF uptake assay performed using the HuTu-80 cell line showed that RF uptake by hRFVT-2 mutant p.P141T was slightly reduced ($P < 0.01$) compared to wild-type hRFVT-2, whereas RF uptake by hRFVT-3 mutant p.N21S was drastically reduced ($P < 0.001$) than the wild-type hRFVT-3 (Fig. 3), and almost equivalent to the basal levels obtained with the cells transfected with GFPC3 empty vector.

3.5. Live cell confocal imaging studies

Membrane targeting and trafficking studies based on live-cell confocal imaging of HuTu-80 cells transiently transfected with mutant GFP-hRFVT-2[P141T] showed membranous expression similar to wild-type GFP-hRFVT-2. The clinical mutant GFP-hRFVT-3[N21S], however, exhibited no expression in the cell surface and was retained in intracellular vesicles unlike wild-type GFP-hRFVT-3 (Fig. 4A). Furthermore, co-transfection of the intracellularly retained construct GFP-hRFVT-3[N21S] with an endoplasmic reticulum marker (DsRed-ER) exhibited significant colocalization within the ER, whereas such an overlap was not observed with cells transfected with wild-type GFP-hRFVT-3 construct (Fig. 4B). Finally, U87 cells expressed with wild-type and mutant constructs showed a membranous distribution pattern similar to that observed in HuTu-80 cells (Supplementary Fig. 1).

4. Discussion

BVVLS, an autosomal recessive and rarely autosomal dominant and X-linked progressive neuronopathy, is inherited by the defective riboflavin transporters mainly and characterized by pontobulbar palsy associated with sensorineural deafness. According to BVVL International, approximately 74 cases have been reported worldwide. Few BVVLS cases have been reported among Indian populations, while the occurrence of mutations in RFVTs from patients and their families has not been diagnosed [12,13]. Here we report on genetic defects in hRFVT-2 and hRFVT-3 in a BVVLS patient, who belongs to consanguineous parents of Indian descent; this patient displayed bulbar palsies, and deafness but no obvious brain abnormalities (as noted by MRI). A consolidated report made recently with the details of 70 BVVLS patients having either RFVT2 or RFVT3 deficiency disclosed that, 16 patients either with RFVT-2 or RFVT-3 deficiency were undergone for MRI, among them only 2 patients with RFVT-3 deficiency showed abnormalities in MRI, while the remaining patients displayed normal MRI [14]. Thus, RFVT deficiency may not necessarily lead to abnormalities in the brain. Biochemical abnormalities like low plasma RF and creatinine levels were also observed. The proband's plasma RF level was found to be markedly lower than the normal range (1.89 μg/L, while normal range is between 3 and 15 μg/L), indicating a state of deficiency in this patient. Previously, plasma riboflavin levels were reported to be

low with no obvious changes in urinary organic acid profile and brain MRI among BVVLS patients having mutations in hRFVT-3 since it is the intestinal specific transporter [15].

Previous studies have shown that the hRFVT-2 is predominantly expressed in the brain [4], while the hRFVT-3 is mainly expressed in intestinal epithelial cells [5]. More recent findings have shown that knocking out RFVT-3 in mouse intestine led to impairment in intestinal RF absorption, as well as RF deficiency and growth retardation and these abnormalities were resolved upon RF supplementation to the knockout animals [16].

In the present study, we report on the identification of defects in both hRFVT-2 and-3 in the same BVVLS patient. A novel missense mutation c.C421A; p.P141T identified in *SLC52A2* has not been reported in any public databases, strongly suggesting that this could be a disease causing mutation in this patient. Likewise, *SLC52A3* sequencing revealed a missense mutation c.A62G; p.N21S, which has been previously reported along with a mutation c.C935A; p.A312V in compound heterozygous state in a BVVLS patient from Iran [17]. However, its functional consequences in RF transport have not been determined thus far. Furthermore, comparative analysis of protein sequences disclosed that both the amino acids in the wild-type hRFVT-2 and hRFVT-3 are highly conserved across species suggesting a strong functional pressure as it may be critical for RF transport function and physiology.

Since, these two mutations were predicted to cause disease by *in silico* analysis using Polyphen and Mutation taster, functional characterization based on ^{3}H-riboflavin uptake studies, and confocal studies were performed using HuTu-80 and U87 cell lines transfected with mutant hRFVT-2 and hRFVT-3 constructs. Studies aimed at demonstrating the functional effect of the identified clinical mutations revealed that ^{3}H-RF uptake by hRFVT-2::p.P141T variant is slightly inhibited. In addition, the distribution pattern of p.P141T variant in the membrane is similar to that of wild-type hRFVT-2, suggesting that reduction in RF uptake may be partly due to conformational changes in the hRFVT-2 polypeptide. However, the hRFVT-3::p.N21S mutant displayed a drastic inhibition in RF uptake and impairment in membrane expression of the mutated protein. These findings suggest that the involved amino acid plays a role in trafficking and targeting of hRFVT-3 to the cell membrane.

As mentioned earlier, the hRFVT-2 is expressed mainly in the brain, and thus, one would expect that dysfunction of this transporter would somehow affect the brain. However, since the patient brain MRI was normal, it is likely that the mild impairment in the function of the hRFVT-2::P141T mutant is not sufficient to be a significant contributor to the disease condition of this patient. On the other hand, the hRFVT-3 is mainly expressed in the intestinal epithelial cells and defective transport function of this transporter lead to impairment in intestinal RF absorption and development of RF deficiency.

In conclusion, a BVVLS patient of Indian origin is diagnosed with two missense mutations, c.421C>A [p.P141T] in hRFVT-2 and c.62A>G [p.N21S] in hRFVT-3. To the best of our knowledge, this is the first report documenting the existence of two mutations in a BVVLS patient, one in the intestinal and the other in the brain specific riboflavin transporters.

Moreover, RFVT-2 and RFVT-3 have not been clinically correlated to any particular symptom and discriminated still now based on the clinical features, biochemical abnormalities, MRI, Neurophysiology and Histopathology [14]. Thus, this study warrants genetic testing for both hRFVT-2 and hRFVT-3, which will serve as a valuable tool for the complete diagnosis of BVVLS. In the future, this approach will benefit the children with early onset of BVVLS and also aid in therapeutic and personalized medicine.

Supplementary Material

Refer to Web version on PubMed Central for supplementary material.

Acknowledgments

We thank Dr. Shunsaku Nakagawa, Kyoto University, Japan for his generous gift of *pcDNA-hRFVT2* construct.

Funding

Authors gratefully acknowledge DST-PURSE (SR/S9/Z-23/2010/28) program, Madurai Kamaraj University, India for the financial support. We are also grateful for the funding from the DVA and NIH grants (DK-56061, DK58057, AA 018071 to HMS; DK107474 to VSS; 5UL1GM118979, 5TL4GM118980, 5RL56M118978 to TT).

Abbreviations

hRFVT	human Riboflavin Transporter
BVVLS	Brown-Vialetto-Van Laere Syndrome
SLC	Solute Carrier
RF	Riboflavin
RFLP	Restriction Fragment Length Polymorphism
DMEM	Dulbecco’s Modified Eagle Medium
HuTu	Human duodenum adenocarcinoma cells
U87	Human brain cells
GFP	Green Fluorescent Protein

References

1. Green P, Wiseman M, Crow YJ, et al. Brown-Vialetto-Van Laere syndrome, a Ponto-Bulbar palsy with deafness, is caused by mutations in C20orf54. Am J Hum Genet. 2010; 86:485–489. [PubMed: 20206331]
2. Hawkins SA, Nevin NC, Harding AE. Pontobulbar palsy and neurosensory deafness (Brown-Vialetto-van Laere syndrome) with possible autosomal dominant inheritance. J Med Genet. 1990; 27:176–179. [PubMed: 2325091]
3. Johnson JO, Gibbs JR, Van Maldergem L, Houlden H, Singleton AB. Exome sequencing in Brown-Vialetto-van Laere syndrome. Am J Hum Genet. 2010; 87:567–569. [PubMed: 20920669]
4. Yao Y, Yonezawa A, Yoshimatsu H, Masuda S, Katsura T, Inui K. Identification and comparative functional characterization of a new human riboflavin transporter hRFT3 expressed in the brain. J Nutr. 2010; 140:1220–1226. [PubMed: 20463145]

5. Fujimura M, Yamamoto S, Murata T, et al. Functional characteristics of the human ortholog of riboflavin transporter 2 and riboflavin-responsive expression of its rat ortholog in the small intestine indicate its involvement in riboflavin absorption. J Nutr. 2010; 140:1722–1727. [PubMed: 20724488]
6. Johnson JO, Gibbs JR, Megarbane A, et al. Exome sequencing reveals riboflavin transporter mutations as a cause of motor neuron disease. Brain. 2012; 135:2875–2882. [PubMed: 22740598]
7. Haack TB, Makowski C, Yao Y, et al. Impaired riboflavin transport due to missense mutations in SLC52A2 causes Brown-Vialetto-Van Laere syndrome. J Inherit Metab Dis. 2012; 35:943–948. [PubMed: 22864630]
8. Ho G, Yonezawa A, Masuda S, et al. Maternal riboflavin deficiency, resulting in transient neonatal-onset glutaric aciduria Type 2, is caused by a microdeletion in the riboflavin transporter gene GPR172B. Hum Mutat. 2010; 32:E1976–E1984.
9. Anand G, Hasan N, Jayapal S, et al. Early use of high-dose riboflavin in a case of Brown-Vialetto-Van Laere syndrome. Dev Med Child Neurol. 2012; 54:187–189. [PubMed: 22098162]
10. Zheng L, Baumann U, Reymond JL. An efficient one-step site-directed and site-saturation mutagenesis protocol. Nucleic Acids Res. 2004; 32:e115. [PubMed: 15304544]
11. Subramanian VS, Rapp L, Marchant JS, Said HM. Role of cysteine residues in cell surface expression of the human riboflavin transporter-2 (hRFT2) in intestinal epithelial cells. Am J Physiol Gastrointest Liver Physiol. 2011; 301:100–109.
12. Puri V, Rohtagi A, Parihar PS. Ponto-Bulbar palsy with deafness (Vialetto-Van Laere syndrome). Indian Pediatr. 1996; 33:140–142. [PubMed: 8772937]
13. Chandran R, Alexander M, Naina P, Balraj A. Auditory neuropathy spectrum disorder with Brown-Vialetto-Van Laere syndrome: challenges in hearing rehabilitation. J Laryngol Otol. 2015; 129:504–508. [PubMed: 25994385]
14. Jaeger B, Bosch AM. Clinical presentation and outcome of riboflavin transporter deficiency: mini review after five years of experience. J Inherit Metab Dis. 2016; 39:559–564. [PubMed: 26973221]
15. Bosch AM, Stroek K, Abeling NG, et al. The Brown-Vialetto-Van Laere and Fazio Londe syndrome revisited: natural history, genetics, treatment and future perspectives. Orphanet J Rare Dis. 2012; 7:83. [PubMed: 23107375]
16. Subramanian VS, Lambrecht N, Lytle C, Said HM. Conditional (intestinal-specific) knockout of the riboflavin transporter-3 (RFVT-3) impairs riboflavin absorption. Am J Physiol Gastrointest Liver Physiol. 2016; 310:285–293.
17. Dezfouli MA, Yadegari S, Nafissi S, Elahi E. Four novel C20orf54 mutations identified in Brown-Vialetto-Van Laere syndrome patients. J Hum Genet. 2012; 57:613–617. [PubMed: 22718020]

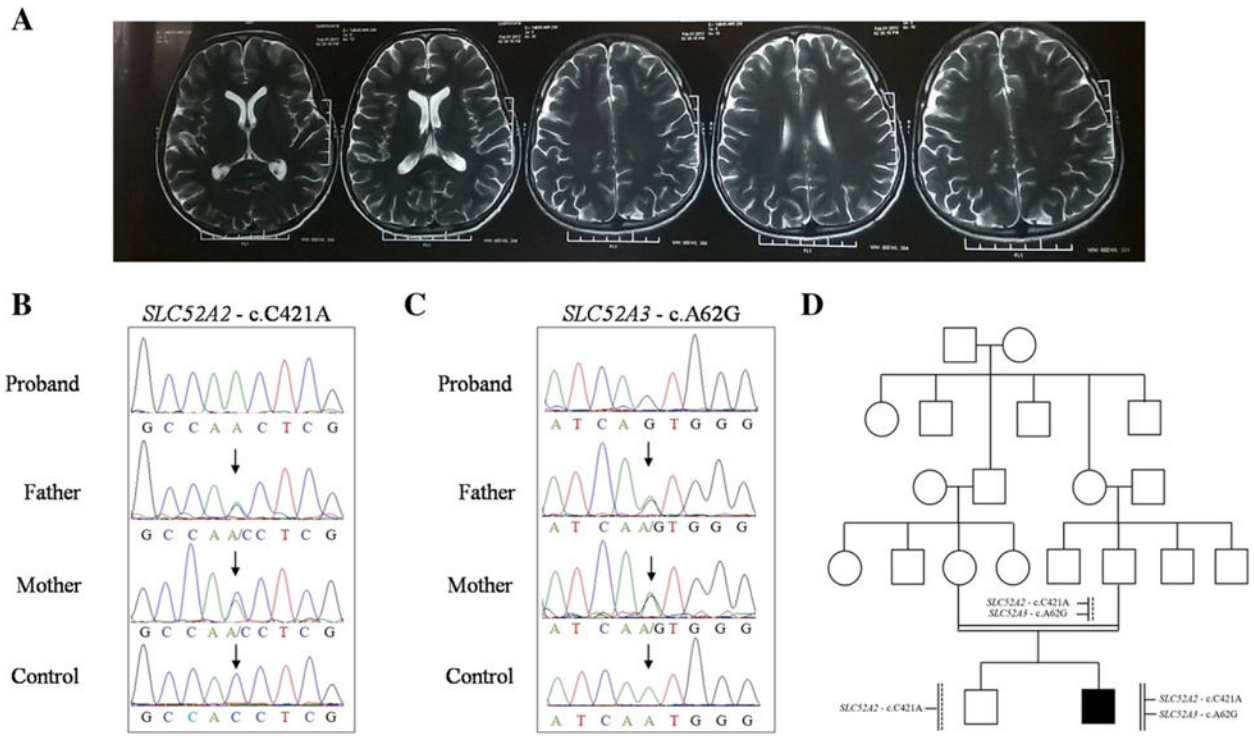

Fig. 1.

Clinical observations & Genetic testing. A) Brain MRI shows the normal appearance of the brain. B) Chromatogram shows the missense mutation *SLC52A2* - c.C421A; p.P141T in BVVLS proband and parents compared with healthy control individual. C) Chromatogram shows the missense mutation *SLC52A3* - c.A62G; p.N21S in BVVLS proband and parents compared with healthy control individual. D) Pedigree of a five generation consanguineous family shows allelic defect of the identified mutations (filled square indicates the proband).

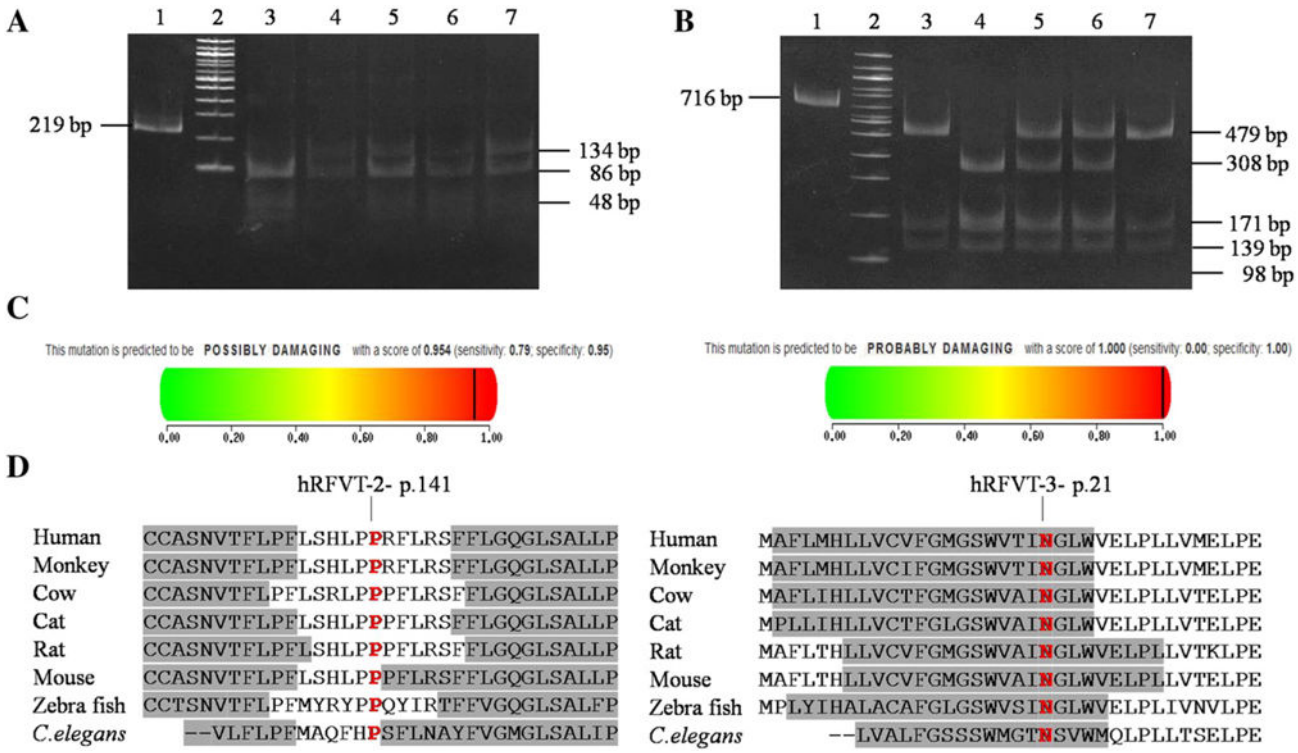

Fig. 2.

Restriction Fragment Length Polymorphism and *In silico* analysis. A) RFLP analysis with *MnlI* for the mutant confirmation in *SLC52A2* - c.C421A; p.P141T. Lane 1: Undigested PCR product, Lane 2: 100 bp DNA ladder, Lane 3: Control, Lane 4: Proband, Lane 5: Father, Lane 6: Mother, Lane 7: Sibling. B) RFLP analysis with *TspRI* for the mutant confirmation in *SLC52A3* - c.A62G; p.N21S. Lane 1: Undigested PCR product, Lane 2: 100 bp DNA ladder, Lane 3: Control, Lane 4: Proband, Lane 5: Father, Lane 6: Mother, Lane 7: Sibling. C) Polyphen analysis shows the structural stability of *SLC52A2* and *SLC52A3* upon mutation. D) Comparison of protein sequence of hRFVT-2 and hRFVT-3 across other species shows the conserved nature of the wild-type residue (Loop region, transmembrane domain and conserved wildtype residues are highlighted in white, grey and red respectively).

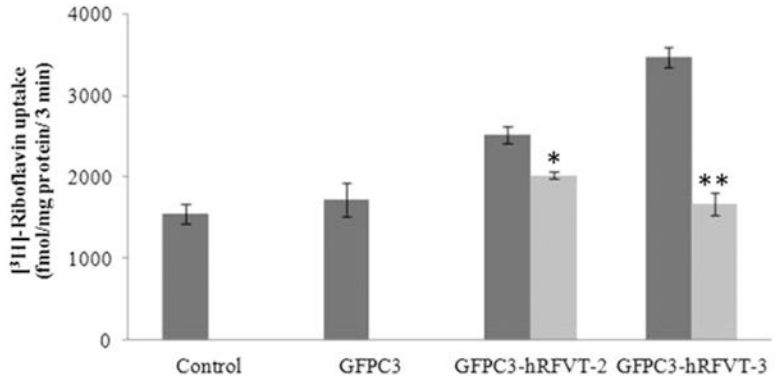

Fig. 3.

Functional characterizations of clinical mutants. RF uptake by HuTu-80 cells transfected with empty vector (GFPC3), wild-type *SLC52A2*, wild-type *SLC52A3*, mutant *SLC52A2* (p.P141T) and mutant *SLC52A3* (p.N21S). After 48 h of transfection, cells were incubated with [^{3}H]-RF (14 nM; pH 7.4) for 3 min at 37 °C and expressed as fmol mg protein^{-1} min^{-1}. Data are means ± SE of 3–5 independent experiments. Data were analyzed by one-way ANOVA followed by Tukey's honestly significant difference (HSD) test, with statistical significance being set at 0.01 (*$P < 0.01$; **$P < 0.001$).

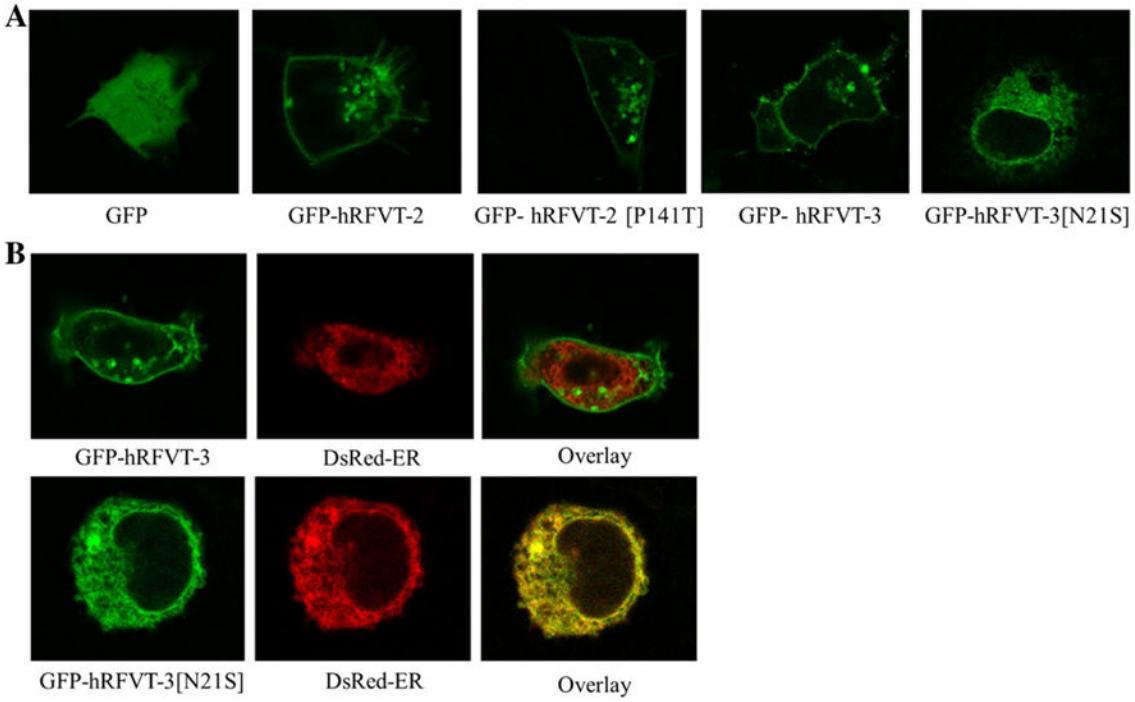

Fig. 4.

Cellular distributions of mutant hRFVT-2 and hRFVT-3 in HuTu-80 cell line. A) Distribution of wild-type and mutant hRFVT-2 and hRFVT-3 in HuTu-80 cell line after 48 h of transfection [lateral (xy) section]. B) Sub-cellular expression of hRFVT-3. HuTu-80 cells grown in glass-bottomed petri dishes were transfected with GFP-hRFVT-3 wild-type and mutant (left) along with DsRed-ER (middle), and the cells were imaged after 48 h of transfection. Data are means ± SE of at least 4 independent experiments.